6-25-1995

Dynamics of Vortices in Superconductors Observed by Electron Waves

Akira Tonomura
Advanced Research Laboratory Hitachi

Follow this and additional works at: https://digitalcommons.usu.edu/microscopy

Part of the Biology Commons

Utah State University
MERRILL-CAZIER LIBRARY

DYNAMICS OF VORTICES IN SUPERCONDUCTORS OBSERVED BY ELECTRON WAVES

Akira Tonomura

Advanced Research Laboratory Hitachi, Ltd., Hatoyama, Saitama 350-03, Japan

Telephone Number: (81) 492-96-6111 (Ext. 216) / FAX number: (81) 492-96-6006

Abstract

Although, in electron microscopy, an object is usually observed by using the intensity of an electron beam transmitted through it, the phase distribution of the electron beam also provides different information about the object. It has been difficult, however, to obtain the phase information because of the low coherence of an electron beam. Recent development of a "coherent" field emission electron beam and related techniques, such as electron holography, has provided a way to observe microscopic objects and fields by precisely measuring the phase information of an electron beam. It has, for example, become possible to observe the dynamics of individual vortices in superconducting thin films.

Introduction

The phase of an electron wave function can now be measured precisely and even in real-time because a "coherent" field-emission electron beam has been developed (see Tonomura, 1993). Fundamental features in quantum mechanics can now be experimentally investigated. We can also observe and measure hitherto invisible objects and fields in a microscopic region by making the best use of the short wavelength of an electron wave. Examples of the former are the proof of the existence of the Aharonov-Bohm effect (Peshkin and Tonomura, 1989) and the demonstration of the single-electron build-up of an interference pattern (Tonomura *et al.*, 1989; see also, Donati *et al.*, 1973; Lichte, 1988). Examples of the latter are the observation of both magnetic domain structures in ferromagnetic thin films (Tonomura *et al.*, 1980) and individual magnetic vortices in superconductors (Harada *et al.*, 1992). In this paper, the observation principle behind magnetic fields by electron phase microscopy is first explained and then recently developed applications for vortex observation are introduced.

Brief History of Electron Interferometry

The wavelength of an electron beam can be on the order of 1/100 Å. Therefore, microscopic objects and fields can be measured or observed by electron interferometry using this small unit of length. A limited number of extremely interesting electron-interference experiments were carried out from the 1950's to 1970's to measure inner and contact potentials (Möllenstedt and Keller, 1957), magnetic fluxons (Lischke, 1969; Boersch *et al.*, 1974), and other quantities (see Missiroli *et al.*, 1981).

These electron-interference experiments required highly skillful techniques since only thermal electron beams of low coherence were available. Difficulties in electron-interference experiments can thus be compared to those of optical-interference experiments using a high-pressure mercury-arc lamp as a light source. Therefore, these experiments were only done in a few laboratories,
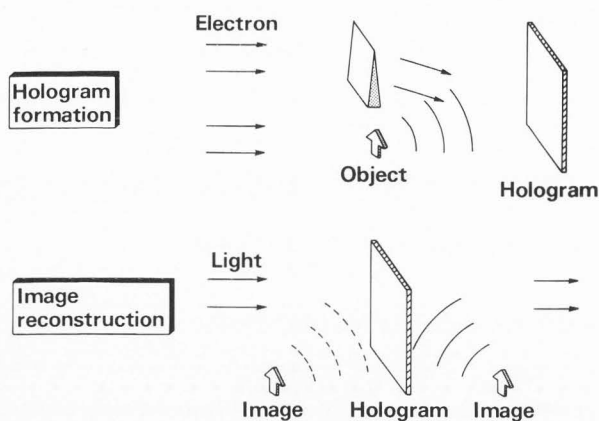
Figure 1. Principle behind electron holography.

----

such as at Tübingen University (Möllenstedt and Keller, 1957), CNRS at Toulouse (Faget and Fert, 1957) and later at Berlin University (Lischke, 1969), Bologna University (Missiroli *et al.*, 1981), Tohoku University (Hibi and Takahashi, 1963), and other places.

A field-emission electron gun was successfully developed by Crewe *et al.* (1968) to form a bright probe for scanning electron microscopes, thus, improving the microscope resolution by one order of magnitude. Several attempts were then made to use this electron beam as a coherent beam (Saxon, 1972; Tonomura and Komoda, 1973; Munch, 1975), and finally, the coherence of an electron beam was improved by two orders of magnitudes (Tonomura *et al.*, 1979); the maximum number of observable interference fringes increased by an order of magnitude, and 50 interference fringes could be observed directly on a fluorescent screen.

This coherent beam has not only made it much easier to carry out electron-interference experiments, but also greatly improved the performance of electron holography (Gabor, 1949) to such an extent that it can be used for practical applications. Since electron wavefronts are faithfully transformed into optical wavefronts through electron holography, versatile optical techniques can be used for electron optics. For example, phase contour maps can be obtained, which was impossible with an electron microscope equipped with an electron biprism (Möllenstedt and Düker, 1956). Furthermore, the precision in phase measurement was increased to $2\pi/100$ using a special technique peculiar to holography (Tonomura *et al.*, 1985).

The recent development of such electron interferometry has made it possible to carry out fundamental experiments in physics that were previously not feasible. In addition, it has engendered new methods of measurement and observation such as the quantitative measurement of the thickness distribution of a uniform material (Tonomura *et al.*, 1985), the magnetic field distribution inside a ferromagnetic film (Tonomura *et al.*, 1980), and the observation of vortices in a superconductor (Matsuda *et al.*, 1989).

Holographic Interference Microscopy

Electron holography (Gabor, 1949) is a two-step imaging process that uses electrons and light (Fig. 1). In the first step, an interference pattern between an object beam and a reference beam is formed in a field-emission transmission electron microscope equipped with an electron biprism and is recorded on film as a hologram.

The hologram is subsequently illuminated by a collimated laser beam and the exact image, or the wavefront, is optically reproduced in one of the two diffracted beams. Another image, a "conjugate image," is produced in the other diffracted beam. Its amplitude is a complex conjugate of the reconstructed image, with the phase value reversed in sign. The first experiment on electron holography was carried out by Haine and Mulvey (1952) followed by Hibi (1956), although reconstructed images were disturbed by conjugate images. In 1968, images free from the effect of conjugate images were first reconstructed using in-line Fraunhofer holography by Tonomura *et al.* (1968) and using off-axis holography by Möllenstedt and Wahl (1968).

An interference micrograph that displays the phase distribution can be obtained by overlapping an optical plane wave with the reconstructed image as a comparison beam in the reconstruction stage of electron holography. If a conjugate image, rather than a plane wave, overlaps this image, the phase difference doubles, as if the phase distribution were amplified by a factor of two. By repeating this technique, a phase shift as small as 1/100th of the electron wavelength can be detected (Tonomura *et al.*, 1985).

Interaction of Electrons with Electromagnetic Fields

To interpret electron-interference micrographs, we must solve the Schrödinger equation in order to determine the interaction of an electron beam with an object. This problem was essentially solved by Aharonov and Bohm (1959), who concluded that an electron wave is influenced, in the form of a phase shift $\Delta\Phi$, by electromagnetic potentials ϕ and A. When the relative change in the potentials is much smaller than 1, on the distance of the electron wavelength, then the $\Delta\Phi$ is given by

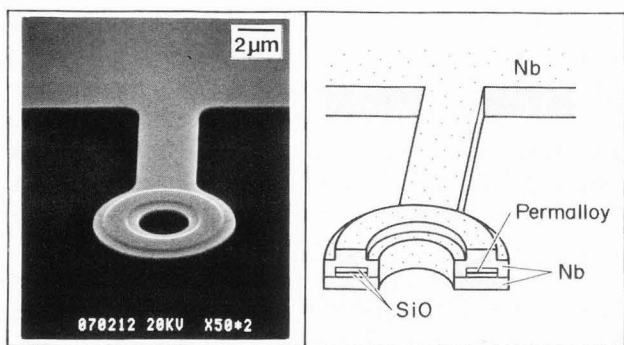$$\Delta\Phi = -(e/\hbar) \int (A ds - \phi dt) \qquad (1)$$

Figure 2. Toroidal permalloy magnets covered with niobium layer. (a) Scanning electron micrograph. (b) Cross-sectional diagram.

Their analysis revealed that two electron waves passing only through field-free regions on both sides of an infinite solenoid can be physically influenced by inaccessible electromagnetic fields, E and B, to produce the observable effect as displacements of the interference fringes.

To be more specific, in a magnetic case, two electron waves enclosing a magnetic flux produce a relative phase shift proportional to the flux, even when the waves never touch the flux (see also Ehrenberg and Siday, 1949). Aharonov and Bohm attributed this effect to the vector potential. The vector potential cannot vanish even in a field-free region surrounding the magnetic flux, since the circulation integral of the vector potential around any loop is equal to the magnetic flux flowing through the loop.

The significance of this effect has recently become evident since it has been regarded as a direct experimental manifestation of the validity of the gauge principle, a guiding principle in the search for a unified theory of all fundamental interactions in nature (Wu and Yang, 1975). However, several theoreticians, for example, Bocchieri and Loinger (1978), questioned the existence of the AB effect and even asserted that it was purely a mathematical concoction, thus producing a controversy (Peshkin and Tonomura, 1989). Previous experimental results were also attributed to flux leakage from the finite solenoids used in these experiments.

Experimental Confirmation of the AB Effect

The crucial experimental point discussed during the AB effect controversy concerned the effect of magnetic flux leakage from finite solenoids on an electron wave. The infinite solenoid assumed in the AB effect theory is experimentally unattainable. However, an ideal geometry can be achieved using a finite toroidal solenoid
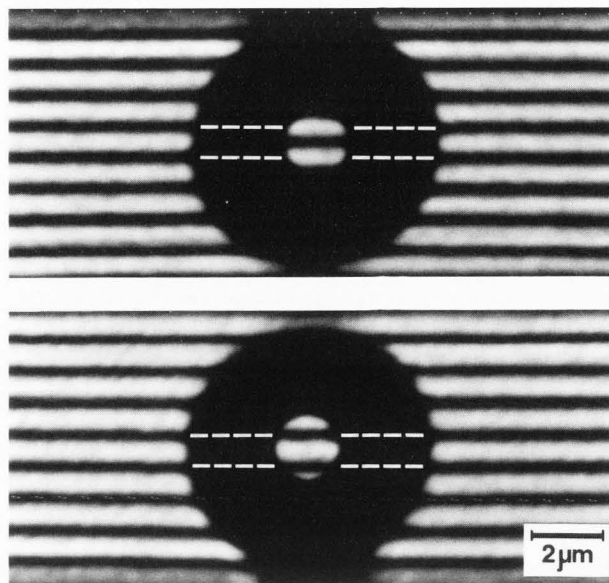

Figure 3. Electron interferograms of toroidal samples at 5 K. (a) $\Delta\Phi = 0$; (b) $\Delta\Phi = \pi$.

(Kuper, 1980). Although toroidal geometry had often been proposed during the controversy, we had to wait for the development of microlithography to be able to fabricate the necessary tiny and complicated samples. We made a series of confirmatory experiments in order to test the existence of the AB effect under various conditions (Peshkin and Tonomura, 1989). The last experiment is described below.

Since no overlap should exist between the electron wave and the magnetic field, tiny toroidal samples were fabricated. The toroidal magnet was covered with a metal layer to prevent electron penetration into the magnet. To avoid even a small amount of flux leakage from the magnet, the metal layer is made of a superconducting material, which prevents magnetic fields passing through because of the Meissner effect.

A scanning electron micrograph of a fabricated sample is shown in Figure 2. Since the magnetic flux cannot be varied, as in the case of a solenoid, many toroidal samples with different magnetic flux values, ranging from $4(h/e)$ to $6(h/e)$, were fabricated.

An electron wave was incident on a toroidal sample cooled to 5 K and the relative phase shift between two electron waves, one passing inside and the other outside the toroidal sample, was measured by means of an interferogram formed by electron holography (Tonomura *et al.*, 1986). Although, many samples with various magnetic flux values were measured, the relative phase shifts detected were either 0 or π (Fig. 3). This quantization of phase shifts is due to the magnetic flux quantization that occurs when a magnetic flux is completely surrounded by a superconductor, and it provides evidence
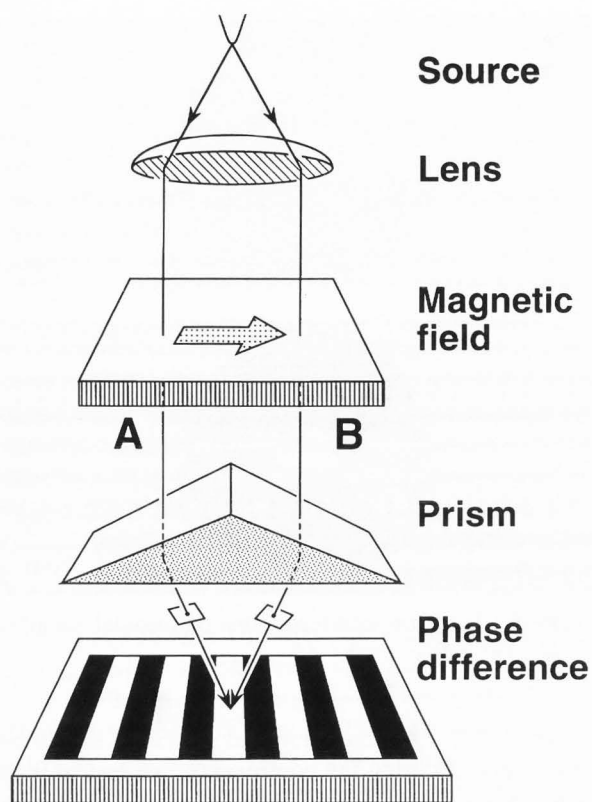
Source

Lens

Magnetic field

A **B**

Prism

Phase difference

Figure 4. Principle of magnetic line observation by interference electron microscopy. A and B indicate two points in the specimen plane.

----

for no leakage flux due to the Meissner effect. Therefore, the conclusion is now obvious. A relative phase shift of π (Fig. 3b), which means that an odd number of flux quanta are trapped in a superconductor, is produced even when the magnetic fields are confined within the superconductor and shielded from the electron wave. This proves conclusively that the AB effect exists. It can be seen from eq. (1) that electromagnetic fields can be observed quantitatively in electron waves as phase shifts. In fact, the development of a "coherent" field-emission electron beam has opened the way for the observation of microscopic electromagnetic fields.

Applications of Interference Microscopy

Magnetic domain structure

The interpretation of an interference micrograph of a ferromagnetic thin film is straightforward. The contour fringes follow the projected magnetic lines of force in h/e flux units. This is easily derived from eq. (1). The relative phase shift $\Delta\Phi$ between two beams starting from a point, passing through two points A and B in the specimen plane and meeting at another point in the observation plane (Fig. 4) is given by the magnetic flux

enclosed by the two electron trajectories. When the two points, A and B, are along a single magnetic line of force, $\Delta\Phi$ vanishes, i.e., the phase contour lines lie along the magnetic lines. When two electron beams, passing through A and B, enclose a flux of h/e, then $\Delta\Phi = 2\pi$. Therefore, a constant magnetic flux of h/e flows between two adjacent contour lines in an interference micrograph.

An example for a hexagonal cobalt particle is shown in Figure 5. No information can be obtained from the electron micrograph, or reconstructed image (Fig. 5a). This is because the sample thickness is uniform and the magnetization has no influence on the intensity of the transmitted electron beam. Information about the magnetization distribution is contained in the phase distribution. In fact, it can be seen from the two-times phase-amplified interference micrograph (Fig. 5b), how magnetic lines of force rotate in such a fine particle. The contour map (Fig. 5b) itself does not allow one to decide whether the magnetization direction is clockwise or counter-clockwise, since these two possibilities correspond to whether the wavefront protrudes like a mountain or is hollow like a valley. This can, however, be decided from the interferogram, (Fig. 5c), which is obtained by slightly tilting two interfering beams in the optical reconstruction stage. The wavefront of the transmitted electron beam is first retarded at the particle edge because of the thickness effect. Then, it is advanced inside the particle because of the magnetic effect. This means that the magnetization direction is clockwise.

It has been difficult to experimentally determine the magnetization distribution in such a fine particle. The magnetic structure is difficult to identify even when observed by Lorentz microscopy, which provides magnetic domain structure information with the highest spatial-resolution currently available. This is because the large defocusing needed for observation of domain structures results in the magnetic contrast overlapping the diffraction pattern of the particle. A Lorentz micrograph of the particle is shown in Figure 5d. This micrograph was optically reconstructed by merely defocusing the reconstructed image from the same electron hologram, which is possible because a hologram contains all the information of the scattered electron wave from an object. Because the outer shape of the particle is completely blurred, as can be seen in Lorentz micrograph (Fig. 5d), it is not easy to predict the magnetization distribution.

Flux quantization process

The process of magnetic flux quantization can be observed directly using the toroidal ferromagnet (Fig. 2) used in the AB effect experiment. Holographic interference microscopy was used to measure, at various temperatures, the relative phase shift between two electron
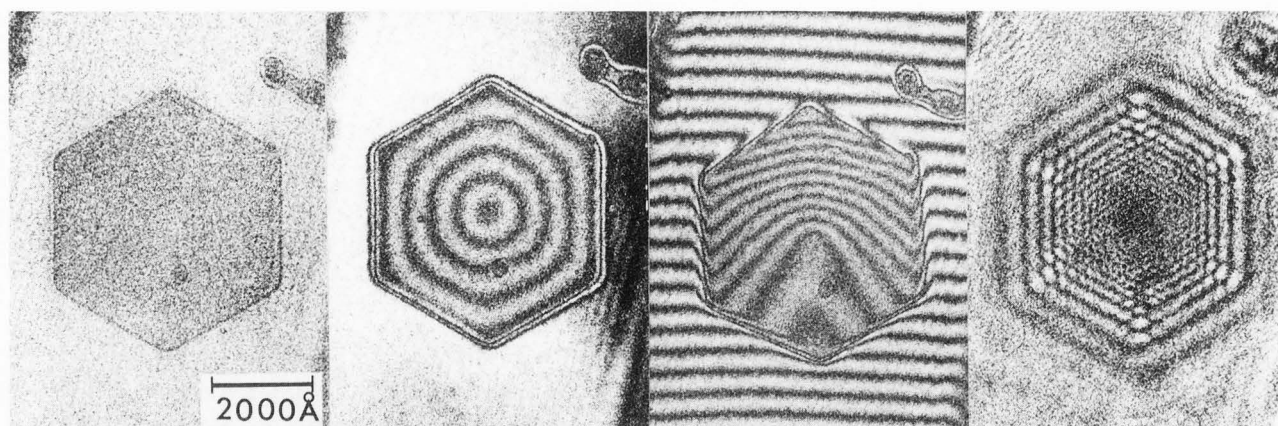
Figure 5. Interference micrograph of hexagonal cobalt particle: (**a**) Reconstructed image; (**b**) Two-times phase-amplified contour map; (**c**) Two-times phase-amplified interferogram; and (**d**) Lorentz micrograph. No contrast can be seen in the reconstructed image (a), whereas in-plane magnetic lines of force are displayed as contour fringes in the contour map (b). The direction of magnetic lines can be determined to be clockwise from the interferogram (c). The Lorentz micrograph (d) can be obtained optically from the hologram, from which it is difficult to determine the magnetic domain structure.
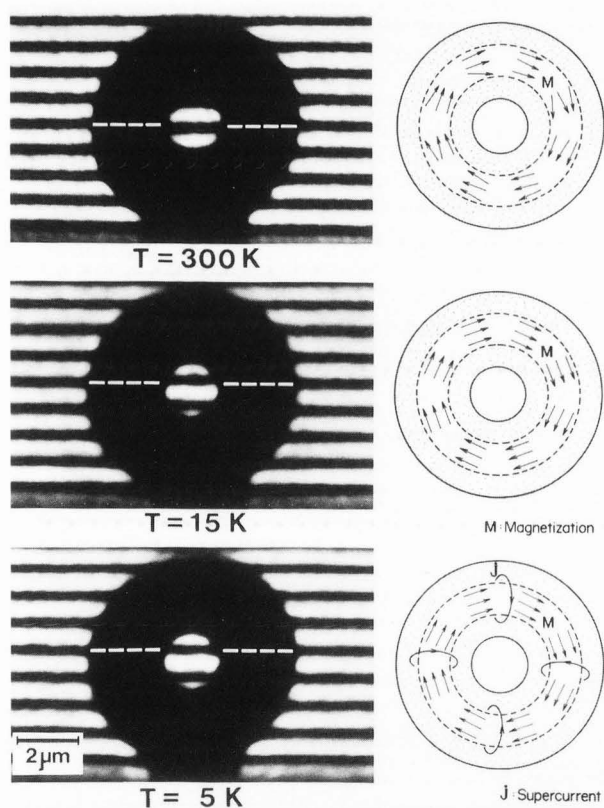

Figure 6. Temperature dependence of electron interferogram of toroidal samples. (**a**) $\Delta\Phi = 0.3\ \pi$ at $T = 300$ K; (**b**) $\Delta\Phi = 0.8\pi$ at $T = 15$ K; (**c**) $\Delta\Phi = \pi$ at $T = 5$ K. M: Magnetization; J: supercurrent.

----

beams, one passing through the hole and the other passing outside the toroidal sample.
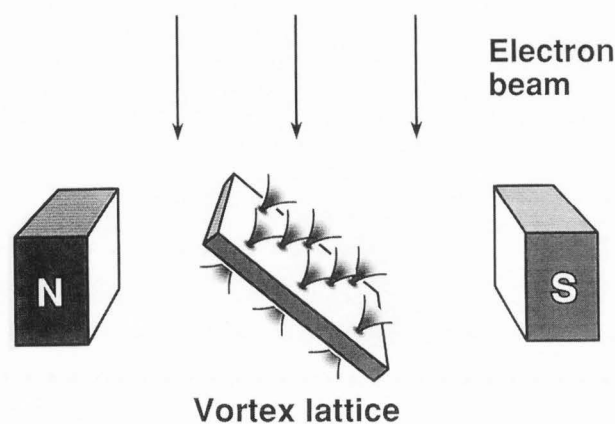
Figure 7. Experimental arrangement for observing magnetic vortices.

An example of this result is shown in Figure 6. The phase shift at room temperature was 0.3π, as shown in Figure 6a. However, when the sample temperature was reduced, the phase shift gradually increased to 0.8π at $T = 15$ K and then jumped to π at Tc (= 9.2 K).

This behavior can be interpreted as follows. Above Tc, the phase shift is determined by the magnetic flux flowing inside the magnet. The temperature dependence of the phase shift from 300 K to 15 K arises from the fact that magnetization in the permalloy increases by 5% due to the decreasing thermal fluctuations of the spins.

When T decreases below Tc, supercurrent begins to flow in the inner surface layer of the hollow superconducting torus, so that the total magnetic flux is an integral multiple of $h/2e$. The phase shift becomes π, since the number of flux quanta trapped in this sample is odd.
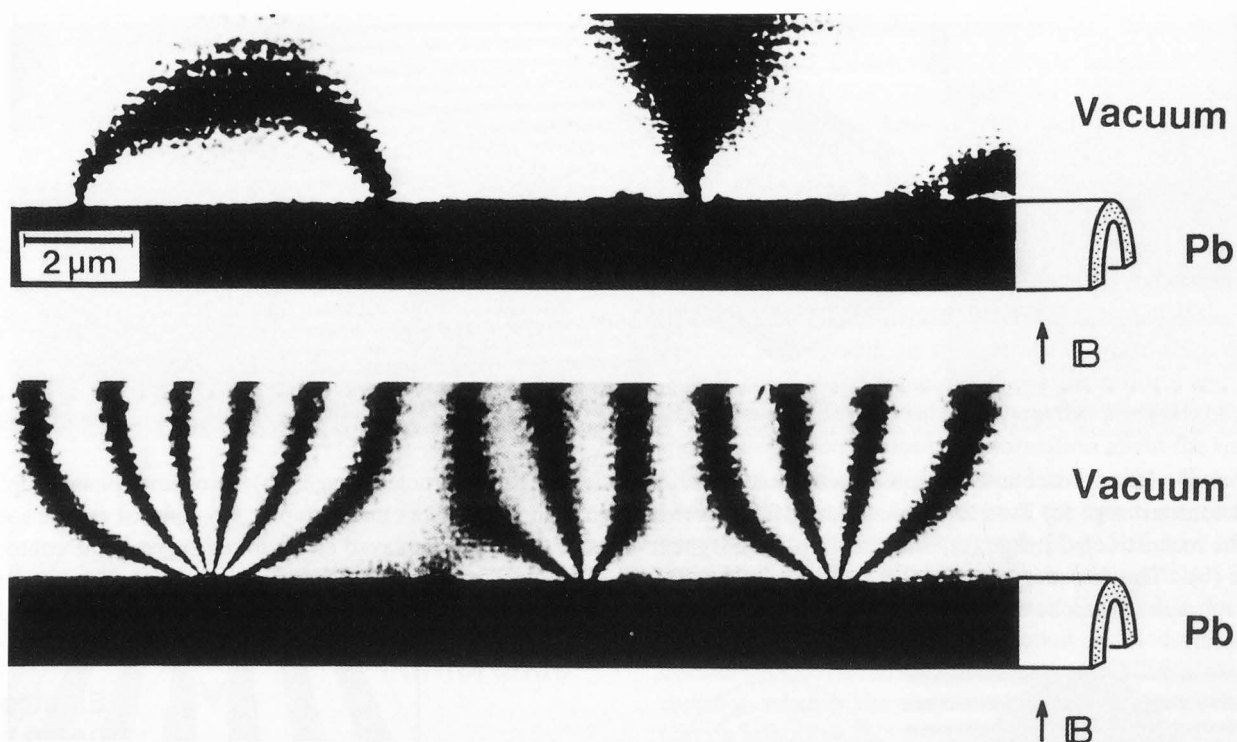
Figure 8. Interference micrographs of magnetic flux leaking from vortices in Pb film (Phase amplification: x 2). **(a)** Thickness = 0.2 μm; **(b)** Thickness = 1 μm.

Magnetic vortices in superconductors

In the previous AB effect experiments, fractional changes in hidden flux quanta could be observed. However, flux quanta or magnetic vortices, penetrating a superconductor, which play an important role in practical superconductivity applications, have evaded direct observation in spite of several attempts. This is because the magnetic flux of a vortex is extremely small ($h/2e = 2 \times 10^{-15}$ Wb), and is the shape of a very thin thread. We attempted to observe vortices by electron holography. At first, we observed vortices by detecting the magnetic flux leaking out from a superconductor surface (Matsuda *et al.*, 1989). The experimental arrangement is shown in Figure 7. A magnetic field of a few G was applied perpendicularly to an evaporated lead film. An electron beam was incident perpendicularly to the magnetic flux penetrating the superconductor and vortices were observed through electron holography.

Figure 8a shows single vortices penetrating a 0.2 μm thick lead film. In this figure, the phase difference is amplified by a factor of two. Therefore, one interference fringe corresponds to one vortex. A single vortex is captured at the right side of this photograph. The magnetic line of force is produced by an extremely small area of the lead surface and spreads out into free space.
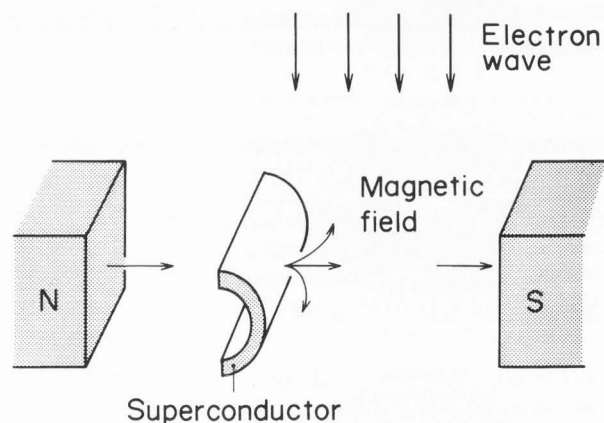

Figure 9. Setup for vortex lattice observation. An external magnetic field of up to 150 G was applied horizontally.

In addition to isolated vortices, we observed a pair of vortices oriented in opposite directions and connected by magnetic lines of force (left side in Figure 8a). One possible reason for the pair production is that when the specimen is cooled to below the critical temperature, the lead becomes superconductive. During the cooling, however, the specimen experiences a state in which the vortex pair appears and disappears repeatedly due to
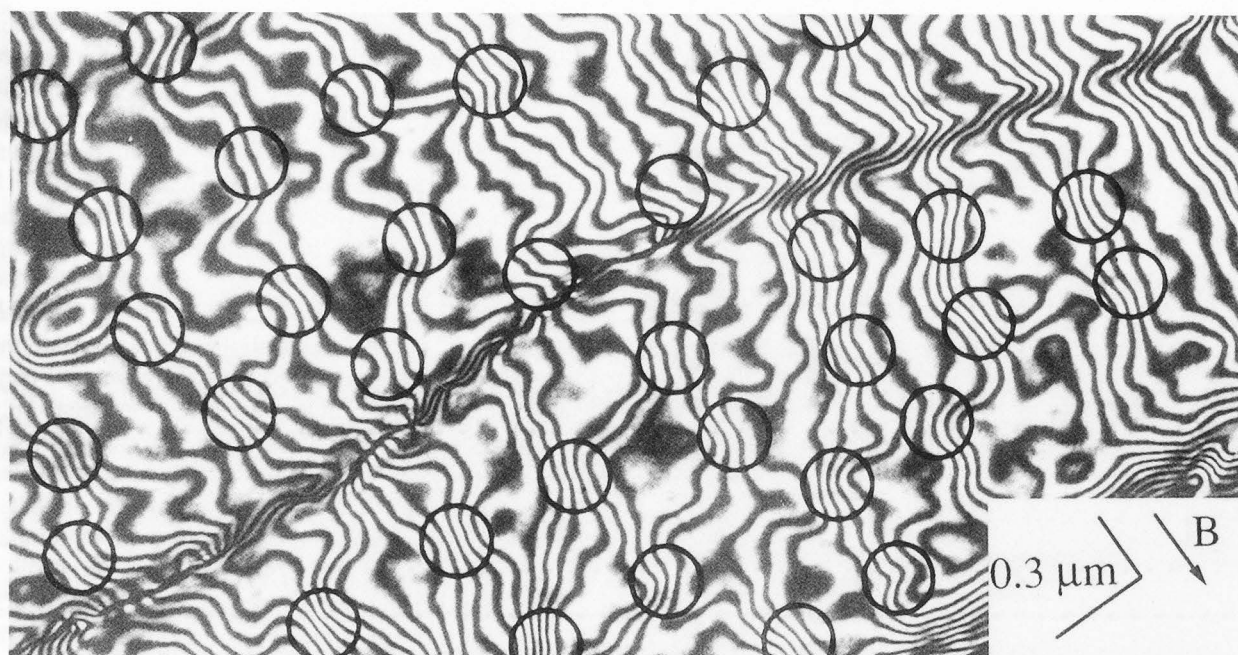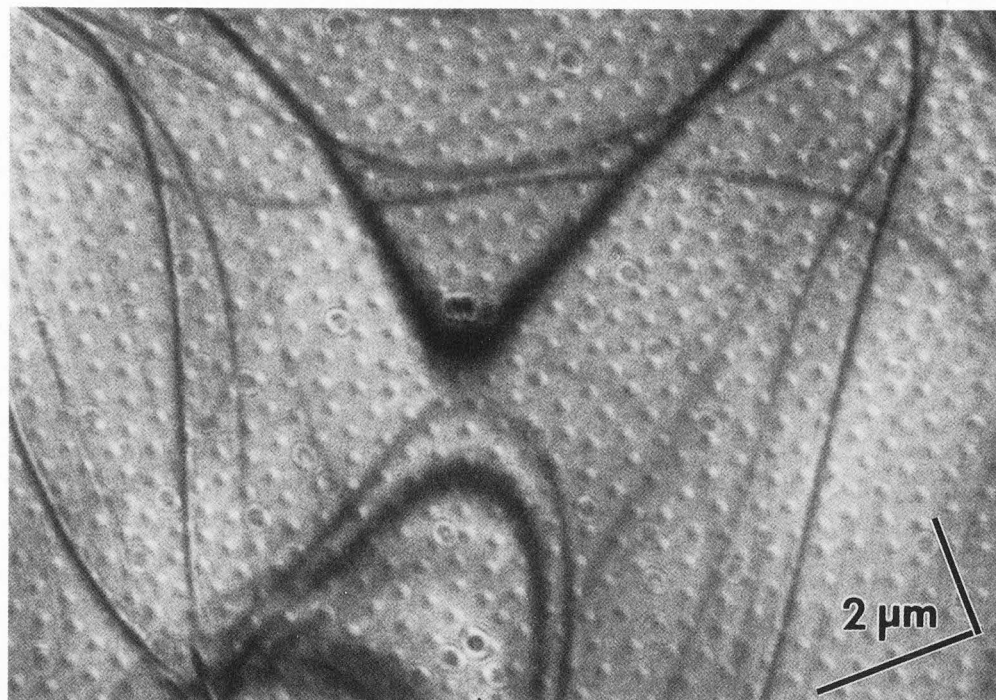
Figure 10 (above). Interference micrograph of a superconducting Nb film at $B = 100$ G (phase amplification: x 16).

Figure 11 (at right). Lorentz micrograph of a two-dimensional array of vortices in a superconducting Nb film at $T = 5$ K and $B = 100$ G.

thermal excitation in a two-dimensional system, and is pinned by some imperfections in the superconductor, eventually resulting in the flux being frozen.

What happens when the thickness of the superconducting thin film is increased? Figure 8b shows the state of the magnetic flux when the thickness is 1 μm. We can see that the state changes completely. Magnetic flux penetrates the superconductor, not as individual vortices, but in bundles. The figure does not show any

vortex pairs.

An explanation for this phenomenon could be that, because lead is a type-I superconductor, the strong magnetic field applied to it partially destroys the superconductive state in some areas of the specimen (intermediate state).

Figure 8b shows that the magnetic flux penetrates those parts of the specimen where superconductivity has been destroyed. However, since the surrounding parts
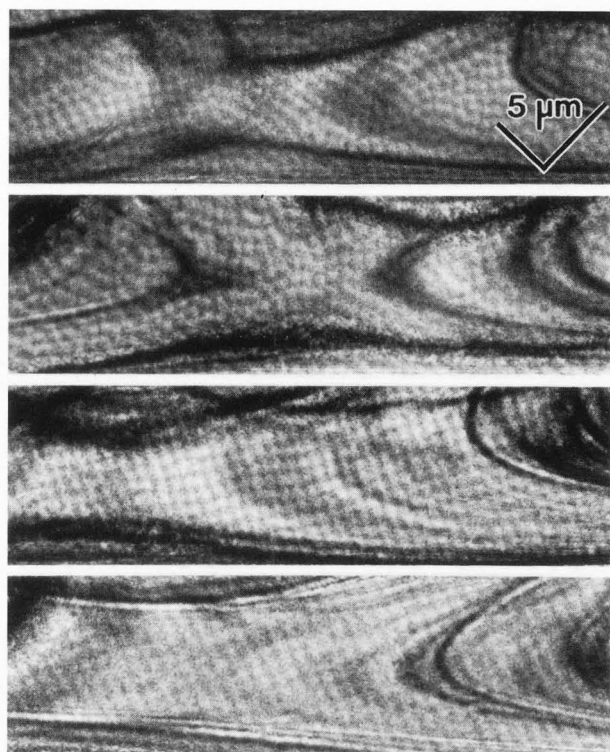
317

Figure 12. Lorentz micrographs of a BSCCO (2212) film at $B = 20$ G: **(a)** $T = 5$ K; **(b)** $T = 20$ K; **(c)** $T = 56$ K; **(d)** $T = 68$ K.

---

are still superconductive, the total amount of penetrating magnetic flux is an integral multiple of the flux quantum, $h/2e$. Thin superconducting films (Fig. 8a) are an exception. The lead behaves like a type-II superconductor and the flux penetrates the superconductor in the form of individual vortices.

In the method described so far, an electron wave is passed near a superconductor surface so that we can observe vortices extending from the surface. With this method, however, we can neither observe a two-dimensional array of vortices nor the inside structure of the superconductor. Recent enhancements in our 350-kV holography electron microscope (Kawasaki *et al.*, 1990), which provides a more "coherent" and more "penetrating" electron wave, have made it possible to observe both the static image of a vortex array by holographic interference microscopy (Bonevich *et al.*, 1993) and their dynamic behavior by Lorentz microscopy (Harada *et al.*, 1992).

The experimental arrangement is shown in Figure 9. A Nb thin film, set on a low-temperature stage, was tilted 45° to an incident beam of 300 kV electrons so that the electrons could be affected by the vortex's magnetic fields.

An example of a vortex array in a single-crystalline Nb thin film (Bonevich *et al.*, 1993) is shown in Figure 10. In this interference micrograph, projected magnetic lines of force can be observed. They become dense in the localized regions indicated by the circles in the photograph, corresponding to individual vortices.

Lorentz microscopy proved useful for observing the dynamic behavior of vortices. In this experiment, the sample was first cooled down to 5 K and the applied magnetic field, B, was gradually increased. When B was increased, vortices suddenly began to penetrate the film. Their number increased as B increased and their dynamic behavior was quite interesting. At first, only a few vortices appeared here and there in the 15 x 10 μm^2 field of view. They oscillated around their own pinning centers and occasionally hopped from one center to another. These movements continued for as long as the vortices remained closely packed ($B \leq 100$ G).

An equilibrium Lorentz micrograph (Harada *et al.*, 1993) at $B = 100$ G is shown in Figure 11. The film has a fairly uniform thickness in the region shown, but is bent along the black curves, called **bend contours**, which are caused by Bragg reflections at the atomic plane. Each spot showing black and white contrast is the image of a single vortex. This contrast reversed, as expected, when the applied magnetic field was reversed. The tilt direction of the sample can be discerned from the line dividing the black and white parts of the spots. Since the black part is on the same side of all the spots, the polarities of all the vortices seen in the region are the same.

A high-T_c superconductor BSCCO (2212) has also been investigated. High-T_c superconductors are difficult to use, practically because the critical current vanishes at high temperatures and under large magnetic fields even when the temperature is well below the critical temperature. This phenomenon probably arises from the behavior of vortices but its exact cause has not yet been determined. Some researchers think that the vortices in high-T_c superconductors melt like molecules in a liquid, making it difficult to fix vortices at pinning sites (Bishop *et al.*, 1992). Evidence for vortex lattice melting was provided by a Bitter figure of BSCCO (2212), in which the vortex image was blurred even at 15 K and 20 G ($Tc = 85$ K) (Kleiman *et al.*, 1989). Other researchers, however, disagree and attribute this phenomenon to weak pinning effects. Accordingly, the practical usable temperature is thought to be not T_c but rather the melting temperature, T_m.

The vortices were dynamically observed to find out whether they actually begin to move under such conditions. The observation was made under a fixed magnetic field (20 G) while increasing the sample temperature from 5 K to above T_c. A Lorentz micrograph at $T = 5$

K is shown in Figure 12a. At 5 K, the vortices were randomly distributed, when the temperature was raised step-wise by a few Kelvins, they began to move. After a few minutes, however, they reached an equilibrium state and became still. They did not melt even at 20 K. At 40-50 K, however, the vortex configuration changed to form a regular lattice. The vortex lattice persisted at higher temperatures, though the image contrast gradually decreased and then disappeared above 77 K.

Conclusions

The performance of electron interferometry has been improved thanks to the development of a coherent field-emission electron beam and electron holography. This technique can be applied to measure the phase distribution of an electron wave interacting with an object to a precision of $2\pi/100$, which opens up a new window for the direct observation of magnetic lines of force in both ferromagnetic and superconductive samples. This technique has a wide range of potential application fields, which will be developed together with an even more coherent electron beam, since the coherence of an electron beam has given a limitation to all aspects of phase measurements, such as in high precision measurements and in real-time observation.

References

Aharonov Y, Bohm D. (1959). Significance of electromagnetic potentials in quantum theory. Phys. Rev. 115, 485-491.

Bishop DJ, Gammel PL, Huse DA, Murray CA. (1992). Magnetic flux-line lattices and vortices in the copper oxide superconductors. Science 255, 165-172.

Bocchieri P, Loinger A. (1978). Nonexistence of the Aharonov-Bohm effect. Nuovo Cimento 47A, 475-483.

Boersch H, Lischke B, Söllig H. (1974). Dynamics of single flux lines in superconducting films by vortex microscopy experiments. phys. stat. sol. (b) 61, 215-222.

Bonevich JE, Harada K, Matsuda T, Kasai H, Yoshida T, Pozzi G, Tonomura A. (1993). Electron holography observation of vortex lattices in a superconductor. Phys. Rev. Lett. 70, 2952-2955.

Crewe AV, Eggeberger DN, Wall DN, Welter LN (1968). Electron gun using a field emission source. Rev. Sci. Instrum. 38, 576-583.

Donati O, Missiroli GF, Pozzi G. (1973). An experiment on electron interference. Am. J. Phys. 44, 639-644.

Ehrenberg E, Siday RE. (1949). The refractive index in electron optics and the principles of dynamics. Proc. Phys. Soc. London B 62, 8-21.

Faget J, Fert C. (1957). Diffraction et inteféreces en optique électronique (Diffraction and interferences in electron optics). Cah. Phys. 83, 285-296.

Gabor D. (1949). Microscopy by reconstructed wave-fronts. Proc. R. Soc. A 197, 454-487.

Haine ME, Mulvey T. (1952). The formation of the diffraction image with electron in the Gabor diffraction microscope. J. Opt. Soc. Amer. 42, 763-773.

Harada K, Matsuda T, Bonevich JE, Igarashi M, Kondo S, Pozzi G, Kawabe U, Tonomura A. (1992). Real-time observation of vortex lattices in a superconductor by electron microscopy. Nature 360, 51-53.

Harada K, Kasai H, Bonevich JE, Yoshida T, Tonomura A. (1993). Vortex configuration and dynamics in $Bi_2Sr_{1.8}CaCuO_x$ thin film by Lorentz microscopy. Phys. Rev. Lett. 71, 3371-3374.

Hibi T. (1956). Pointed filaments (1) Its production and its applications. J. Electron Microsc. 4, 10-15.

Hibi T, Takahashi S. (1963). Electron interference microscope. J. Electron Microsc. 12, 129-133.

Kawasaki T, Matsuda T, Endo J, Tonomura A. (1990). Observation of a 0.055 nm spacing lattice image in gold using a field emission electron microscope. Jpn. J. Appl. Phys. 29, L508-L510.

Kleiman RN, Gammel PL, Schneemeyer LF, Waszczak JV, Bishop DJ. (1989). Reply to Comments on "Evidence from Mechanical Measurements for Flux-Lattice Melting in Single-Crystal $YBa_2Cu_3O_7$ and $Bi_{2.2}Sr_2Ca_{0.8}Cu_2O_8$". Phys. Rev. Lett. 62, 2331.

Kuper CG. (1980). Electromagnetic potential in quantum mechanics: A proposed test of the Aharonov-Bohm effect. Phys. Lett. 79A, 413-416.

Lichte H. (1988). Electron interferometry applied to objects of atomic dimensions. In: New Techniques and Ideas in Quantum Measurement Theory. Greenberger DM (ed.). New York Academy of Sciences, New York. pp. 175-189.

Lischke B. (1969). Direct observation of quantized magnetic flux in a superconducting hollow cylinder with electron interferometer. Phys. Rev. Lett. 22, 1366-1368.

Matsuda T, Hasegawa S, Igarashi M, Kobayashi T, Naito M, Kajiyama H, Endo J, Osakabe N, Tonomura A, Aoki R. (1989). Magnetic field observation of single flux quantum by electron-holographic interferometry. Phys. Rev. Lett. 62, 2519-2522.

Missiroli GF, Pozzi G, Valdrè U. (1981). Electron interferometry and interference electron microscopy. J. Phys. E: Sci. Instrum. 14, 649-671.

Möllenstedt G, Düker H. (1956). Beobachtungen und Messungen an Biprisma-Interferenzen mit Elektronenwellen (Observation and measurement of biprism interferences with electron waves). Z. Phys. 145, 377-397.

Möllenstedt G, Keller M. (1957). Elektroneninterferometrische Messung des inneren Potentials (Electron-interferometric measurement of inner potentials). Z. Physik **148**, 34-37.

Möllenstedt G, Wahl H. (1968). Elektronen-holographie und Rekonstruktion (Electron holography and reconstruction). Naturwiss. **55**, 340-341.

Munch J. (1975). Experimental electron holography. Optik **43**, 79-99.

Peshkin M, Tonomura A. (1989). The Aharonov-Bohm Effect. Lecture Notes in Physics. Vol. 340. Springer-Verlag, Heidelberg. pp. 101-136.

Saxon G. (1972). The compensation of magnetic lens wavefront aberrations in side-band holography with electrons. Optik **315**, 359-375.

Tonomura A. (1993). Electron Holography. Springer Series in Optical Sciences. Vol. 70. Springer-Verlag, Heidelberg. pp. 31-37 and 69-72.

Tonomura A, Fukuhara A, Watanabe H, Komoda T. (1968). Optical reconstruction of image from Fraunhofer electron hologram. Jpn. J. Appl. Phys. **7**, 295.

Tonomura A, Komoda T. (1973). Field emission electron microscope. J. Electron Microsc. **22**, 141-147.

Tonomura A, Matsuda T, Endo J, Todokoro H, Komoda T. (1979). Development of a field emission electron microscope. J. Electron Microsc. **28**, 1-11.

Tonomura A, Matsuda T, Endo J, Arii T, Mihama K. (1980). Direct observation of fine structure of magnetic domain walls by electron holography. Phys. Rev. Lett. **44**, 1430-1433.

Tonomura A, Matsuda T, Kawasaki T, Endo J, Osakabe N. (1985). Sensitivity-enhanced electron-holographic interferometry and thickness-measurement applications at atomic scale. Phys. Rev. Lett. **54**, 60-62.

Tonomura A, Osakabe N, Matsuda T, Kawasaki T, Endo J, Yano S, Yamada H. (1986). Evidence for Aharonov-Bohm effect with magnetic field completely shielded from electron wave. Phys. Rev. Lett. **56**, 792-795.

Tonomura A, Endo J, Matsuda T, Kawasaki T, Ezawa H. (1989). Demonstration of single-electron buildup of an interference pattern. Amer. J. Phys. **57**, 117-120.

Wu TT, Yang CN. (1975). Concept of non-integrable phase factors and global formulation of gauge fields. Phys. Rev. D **12**, 3845-3857.

Discussion with Reviewers

P.W. Hawkes: Do you anticipate that new results can also be expected by applying analogous techniques to ferroelectrics? Are there unsolved problems there, or indeed, with other types of material, to which electron holography and holographic interference microscopy can be expected to contribute?

Author: Such an attempt has been made by Zhang *et al.* (1992). We also tried to observe domain structures of ferroelectric materials, but so far have not been successful. I think the reason why this is difficult, compared to the observation of magnetic field, could be as follows: Even if electric charges exist, they are easily surrounded and shielded by opposite charges, which makes them difficult to observe.

J.C.H. Spence: Equation 1 holds only for weak electrostatic potentials; for stronger projected potentials (e.g., inside a thin crystal), multiple scattering becomes important and eq. (1) cannot be used. Is there any experimental evidence for the failure of eq. (1) due to multiple scattering by the vector potential A? If so, does the AB effect ignore the possibility of multiple scattering?

Author: This is a very interesting question which I have never thought of. In case of magnetic fields leaking out of a magnetic head, for example, we met with the case where the approximation was not valid. In this case, the magnetic fields deflected incident electrons so greatly that the intensity was not constant even in the in-focus image. However, in case of the AB effect, electrons are not deflected and, therefore, the intensity change will never occur. But, in case of a large magnetic flux enclosed within the superconductor, the effect of multiple scattering may happen. We have only measured a rather small flux on the order of 10 ($h/2e$), and, consequently, we have not detected such an effect. I am glad to know what kinds of effects are theoretically expected to occur in this case.

Additional Reference

Zhang X, Hashimoto H, Joy DC. (1992). Electron holography of ferro-electric domain walls. Appl. Phys. Lett. **60**, 784-786.